Supplementary information for

Towards the *n*-type 4V-class Organic Lithium-ion Cathodes: The Case of Conjugated Triflimides and Cyanamides

Xiaolong Guo[1][§], Petru Apostol[1][§], Xuan Zhou[2], Jiande Wang[1], Xiaodong Lin[1], Darsi Rambabu[1], Mengyuan Du[1], Süleyman Er[2] and Alexandru Vlad[1] *

[1] Institute of Condensed Matter and Nanosciences, Molecular Chemistry, Materials and Catalysis, Université catholique de Louvain, Louvain-la-Neuve B-1348, Belgium

[2] DIFFER – Dutch Institute for Fundamental Energy Research, De Zaale 20, 5612 AJ Eindhoven, The Netherlands

[§] These authors contributed equally to this work

* Corresponding author : alexandru.vlad@uclouvain.be

Experimental section

Materials

Benzoyl chloride (>98%), *p*-phenylenediamine (>99%), 2,5-dichloro-1,4-phenylenediamine (>98%), and bis(trimethylsilyl)carbodiimide (98%) were purchased from TCI. Ammonium thiocyanate (>99%, extra pure) and lead (IV) acetate trihydrate were purchased from FisherSci. 2,5-Dichlorocyclohexa-2,5-diene-1,4-dione (95%), *p*-Benzoquinone (99%), trifluoromethanesulfonic anhydride (98%), and Benzene-1,2,4,5-tetraamine tetrahydrochloride (95%) were purchased from Fluorochem. Lithium methoxide (98%), titanium tetrachloride (99.9%), and 2,5-difluoro-1,4-phenylenediamine dihydrochloride (95%) were purchased from Sigma-Aldrich. The glass fiber separator (2325, GF/D) was purchased from Whatman. Li-metal chips, coin cell assembly parts (stainless steel, SS-316), conductive carbon, and polytetrafluoroethylene (PTFE) were purchased from TOB New Energy Technology Co., Ltd. (Xiamen, China). The LP30 (1 M $LiPF_6$ in EC/DMC 1:1 vol%) electrolyte and LiTFSI (battery grade) were purchased from DoDochem (Suzhou, China). The LiTFSI: PYR14-TFSI = 1:9 (mol ratio) electrolyte was purchased from Solvionic (Toulouse, France).

Physico-chemical Characterization

Fourier-transform infrared spectroscopy (FTIR) measurements were carried out using an Agilent Technologies Cary 630 FTIR operated in ATR mode, measured in the wavenumber range from 4000 cm^{-1} to 650 cm^{-1} at a resolution of 4 cm^{-1} with 64 scans. Nuclear Magnetic Resonance (NMR) spectra were recorded with a Bruker magnet system 300 MHz/54 mm ultrashield spectrometer. ^1H chemical shifts are reported in ppm downfield from internal chloroform-d ($\delta = 7.26$ ppm) or DMSO-d6 ($\delta = 2.50$ ppm). High-resolution ESI mass spectra was determined using Thermo Scientific™ Q-Exactive Orbitrap mass spectrometer with APCI+ ionisation mode. The air stability tests were performed under conditions of 10 g/m^3 absolute humidity at a temperature

of 25°C.

Electrochemical measurements

CR2032-type coin cells consisting of the positive electrode and the lithium negative electrode separated by a Celgard 2325 microporous membrane were used for cycling tests. Li_2-PDFSA positive electrode was prepared by mixing the active material with 40 wt.% super P carbon and 10 wt.% polytetrafluoroethylene (PTFE) binder. Other positive electrode materials were mixed with 40 wt.% ketjen black carbon and 10 wt.% polytetrafluoroethylene (PTFE) binder, then pressed onto the coin-cell positive case. All positive electrodes were prepared utilizing a solvent-free dry method. The electrolyte was the 7M $LiN(CF_3SO_2)_2$ (LiTFSI) solution in a mixed solvent of ethylene carbonate (EC) and dimethyl carbonate (DMC) (1:1 by volume) for Li_2-PDFSA, Li_2-DC-PDFSA, and Li_2-DF-PDFSA. The LP30 (1 M $LiPF_6$ in EC/DMC 1:1 vol%) electrolyte was for Li_4-PTFSA cells. LiTFSI: PYR14-TFSI = 1:9 (mol ratio) was used for the cyanamide family. The cells were assembled in an argon-filled glove box. The charge-discharge experiments were performed on the Neware battery test system.

Liquid cyclic voltammetry measurements

Cyclic voltammetry was conducted with a BioLogic Science Instruments SP-300. A three-electrode system with screen-printed platinum as the working and counter electrodes and screen-printed Ag as the pseudo-reference electrode was used for measurements. The 0.1M LiCl in THF or 0.1M LiCl in DMSO were used as supporting electrolytes for the triflimides and cyanamides series, respectively. Then, 3 mM of the active material was dissolved in the electrolyte solution. The CV was measured at a scan rate of 100 mVs^{-1}. After the test, ferrocene was added to the solution and used as an internal reference.

Ex-situ HNMR analyses

Li$_2$-DC-PDCA. A 30 wt.% Li$_2$-DC-PDCA, 10 wt.% PTFE, and 70 wt.% ketjen black electrode was first cycled at a rate of C/15. The electrode material at different SoC and DoD was washed with diethyl ether and dried at 80 °C under vacuum for 3 hours. Then the charged composition was extracted with chloroform-d, and the filtrate was collected for ^{1}H NMR analysis. The composition after one full charge-discharge cycle was extracted with DMSO-d$_6$, and the filtrate was collected for ^{1}H NMR measurement.

Li$_2$-DC-PDFSA. 50wt.% Li$_2$-DC-PDFSA and 50wt.% ketjen black were mixed and cycled at a rate of C/10. The electrode material after one full charge - discharge cycle was washed with diethyl ether and dried at 80 °C under vacuum for 3 hours. The charged material was dried at 80 °C under vacuum for 3 hours then extracted with chloroform-d, and the filtrate was collected for ^{1}H NMR analysis. The compound after one full charge-discharge cycle was extracted with by DMSO-d$_6$, and the filtrate was collected for ^{1}H NMR analysis.

Computational methods

All the simulations were implemented in Schrödinger Materials Science Suite (SMSS) [1]. The three-dimensional geometries of seven studied molecules were first generated using the Maestro editor in SMSS. Then, all the geometries were pre-optimized using the OPLS3e [2] force field (FF) with the aim of finding the lowest energy conformers. The MacroModel [3] package in SMSS was employed for FF. The structural optimizations and single-point calculations were sequentially performed using the Jaguar [4] program in SMSS. The B3LYP-D3 [5] functional and LACVP^{++**} [6] basis set with diffuse and polarization functions were applied for DFT-based optimizations and energetic calculations. The changes in energy and root-mean-square (RMS) density matrix were set at 5×10^{-5} and 5×10^{-6} Hartree, respectively. The default settings of

'Medium' and 'Quick' were chosen for grid density and accuracy level in DFT optimizations, while 'Fine' and 'Accurate' were used in DFT single-point calculations. The log Ka prediction was performed in Jaguar pKa [7] program, as implemented in SMSS. Moreover, an implicit aqueous environment within the standard Poisson–Boltzmann Formalism (PBF) [8] model was used for the log Ka prediction.

Synthesis Procedures

Synthesis of N, N'-(1,4-phenylene) bis(1,1,1-trifluoromethanesulfonamide) (H$_2$-PDFSA)

Triethylamine 4.25 g (42 mmol) of and 2.16 g (20 mmol) of *p*-phenylenediamine were added to 100 mL of anhydrous dichloromethane. The trifluoromethanesulfonic anhydride (1.19 g, 42 mmol) was then added dropwise to the solution at -78 °C for 30 minutes. After addition, the reaction was left to warm up to room temperature and stirred overnight. The obtained suspension was then filtered, and the filtrate was diluted with water and extracted three times with DCM. The red product was obtained by rotary evaporation of the organic layer. ^{1}H NMR (DMSO-d$_6$): δ = 11.93 ppm (br, 2 H, NH), 7.31 ppm (s, 4 H, CH$_{arom}$), IR: 3272 (NH), 1505 (benzene ring). HRMS (ESI) calcd for C$_8$H$_6$F$_6$N$_2$O$_4$S$_2$ [M-H]$^-$: 370.97, found: 370.96. Additional details are shown in **Figure S1**.

Synthesis of N, N'-(2,5-dichloro-1,4-phenylene) bis(1,1,1-trifluoromethanesulfonamide) (H$_2$-DC-PDFSA)

Triethylamine (18 mmol, 1.821 g) and 2,5-dichloro-1,4-phenylenediamine (6 mmol, 1.06 g) were added to 36 mL anhydrous dichloromethane. Then, the trifluoromethanesulfonic anhydride (26.4 mmol, 7.44 g) was added to the solution

dropwise at -30 °C within 10 minutes. After the addition, the reaction was allowed to warm to room temperature and stirred overnight. The suspension was filtered, and the filter residue was washed with dichloromethane to obtain the light brown product. ^{1}H NMR (DMSO-d_6): δ = 11.23 (br, 2 H, NH), 7.44 (s, 2 H, CH$_{arom}$) ppm, IR: 3272 (NH), 1487 (benzene ring). HRMS (ESI) calcd for $C_8H_4Cl_2F_6N_2O_4S_2$ [M-H]$^-$: 438.89, found: 438.88. Additional details are shown in **Figure S2**.

Synthesis of N, N'-(2,5-difluoro-1,4-phenylene) bis(1,1,1trifluoromethanesulfonamide) (H$_2$-DF-PDFSA)

Triethylamine (6 mmol, 607.2 mg) and 2,5-difluorobenzene-1,4-diamine dihydrochloride (1 mmol, 217 mg) were added to 12 mL anhydrous dichloromethane. Then the trifluromathanesulfonic anhydride (12 mmol, 3.38 g) was added dropwise to the solution at -30 °C within 10 minutes. After addition, the reaction was left to warm up to room temperature and stirred overnight. The suspension was filtered, and the filter residue was washed with dichloromethane to get the light pink product. ^{1}H NMR (DMSO-d_6): δ = 11.08 (br, 2 H, NH), 7.34 (t, 2 H, CH$_{arom}$) ppm, IR: 3261 (NH), 1509 (benzene ring). HRMS (ESI) calcd for $C_8H_4F_8N_2O_4S_2$ [M-H]$^-$: 406.95, found: 406.94. Additional details are shown in **Figure S3**.

Synthesis of N, N', N''-(5-((trifluoromethyl) sulfonamido) benzene-1,2,4-triyl) tris(1,1,1-trifluoromethanesulfonamide) (H$_4$-PTFSA)

Triethylamine (8 mmol, 809.6 mg) and 1,2,4,5-benzenetetramine tetrahydrochloride (1 mmol, 284 mg) were added to 36 mL anhydrous chloroform under argon. Then the trifluromathanesulfonic anhydride (10 mmol, 2.82 g) was added dropwise to the solution at -30 °C within 20 minutes. After the addition, the reaction was maintained at -30 °C for 40 minutes, then heated to 60 °C under argon. After two days, 1 mL of diluted acetic acid in 5 mL of chloroform were added. Subsequently, the solvent was evaporated under reduced pressure, and the residue was dissolved using

ethyl acetate. The mixture was washed with 1M HCl aq., and the combined extracts were dried over Na_2SO_4 and filtered through a pad of celite. The filtrate was concentrated in vacuo and washed by hexane to get the reddish product. ^{1}H NMR (DMSO-d_6): δ = 8.75 (br, 4 H, NH), 7.27 (s, 2 H, CH$_{arom}$) ppm, IR: 3298 (NH), 1517 (benzene ring). Additional details are shown in **Figure S4**.

Lithiation of H₂-PDFSA, H₂-DC-PDFSA, H₂-DF-PDFSA and H₄-PTFSA.

Lithiation of H_2-PDFSA, H_2-DC-PDFSA, H_2-DF-PDFSA, and H_4-PTFSA was performed in anhydrous diethyl ether with a stoichiometric amount of lithium hydride. The mixture was stirred at room temperature inside an argon-filled glove box for 2 days. The precipitate was filtered and transferred into a BUCHI glass oven for drying. The Li_2-PDCA, Li_2-DC-PDCA, and Li_2-DF-PDCA were all dried for 14 hours at 140 °C under vacuum. Li_4-PTFSA was dried for 3 hours at 130 °C under vacuum.

For Li_2-PDFSA, ^{1}H NMR (DMSO-d_6): δ = 6.63 (s, 4 H, CH$_{arom}$) ppm, IR: 1506 (benzene ring). 1278, 1017 (SO$_2$).

For Li_2-DC-PDFSA, ^{1}H NMR (DMSO-d_6): δ = 7.12 (s, 2 H, CH$_{arom}$) ppm, IR: 1479 (benzene ring). 1276, 1013 (SO$_2$).

For Li_2-DF-PDFSA, ^{1}H NMR (DMSO-d_6): δ = 6.74 (t, 2 H, CH$_{arom}$) ppm, IR: 1502 (benzene ring). 1274, 1006 (SO$_2$).

For Li_4-PTFSA, ^{1}H NMR (DMSO-d_6): δ = 7.19 (2, 2 H, CH$_{arom}$) ppm, IR: 1498 (benzene ring), 1252, 1002 (SO$_2$).

Additional details are shown in **Figures S1-S4**.

Synthesis of 1,4-phenylene dicyanamide (H₂-PDCA) and 1,4-dicyanamido-2,5-dichlorobenzene (H₂-DC-PDCA)

H_2-PDCA and H_2-DC-PDCA were prepared according to Aquino's paper. [9] The detailed procedure is described below.

Benzoyl chloride (14 g, 0.1 mol) dissolved in 100 mL dried acetone was added dropwise to a refluxing ammonium thiocyanate (7.6 g, 0.1 mol) solution in 100 mL acetone with magnetic stirring. After finishing adding benzoyl chloride solution, the mixture was refluxed for 5 minutes to ensure complete formation of benzoyl isothiocyanate. Then 100 mL acetone solution of *p*-phenylenediamine (5.4 g, 0.05 mol) was added dropwise to the refluxing reaction mixture to precipitate thiourea derivatives. After the addition was completed, the reaction mixture was refluxed for another 15 minutes and hot filtered. The light yellow thiourea derivative was washed with acetone, water, and again acetone and dried under vacuum at room temperature. The thiourea derivative was dissolved in 250 mL 2.5 M NaOH solution by boiling for 10 minutes. When the solution was cooled to 65 °C, 100 ml aqueous solution of lead (II) acetate trihydrate (37.9 g, 0.1 mol) was slowly added with magnetic stirring, and black lead sulfide precipitated immediately. The reaction mixture was stirred at 65 °C for another 5 minutes and then filtered. The filtrate was cooled in an ice bath, and 30 mL glacial acetic acid was added for neutralization while a precipitate formed. The white product was filtered out and washed with plenty of water until neutral pH was attained. For H_2-PDCA, ^{1}H NMR (DMSO-d$_6$): δ = 6.94 (s, 4 H, CH$_{arom}$) ppm, IR: 3380, 3168 and 3104 (N-H), 2221 (CN), 1528 (benzene ring). HRMS (ESI) calcd for $C_8H_6N_4$ [M-H]$^-$: 157.06, found: 157.05.

Additional details are shown in **Figure S5**.

The synthesis of H_2-DC-PDCA follows essentially identical procedures as H_2-PDCA. For H_2-DC-PDCA, ^{1}H NMR (DMSO-d$_6$): δ = 7.21 (s, 2 H, CH$_{arom}$), 10.14 (br, 2 H, NH) ppm, IR: 3157 (N-H), 2228 (CN), 1513 (benzene ring). HRMS (ESI) calcd for $C_8H_4Cl_2N_4$ [M-H]$^-$: 224.98, found: 224.97.

Additional details are shown in **Figure S6**.

Synthesis of 1,4-dicyanamido-2,5-difluorobenzene (H₂-DF-PDCA)

Benzoyl chloride (616 mg, 4.4 mmol) dissolved in 6 mL dried acetone was added dropwise to the refluxing ammonium thiocyanate (304 mg, 4 mmol) in 7 mL acetone with magnetic stirring. After benzoyl chloride addition, the mixture was refluxed for 1 hour to ensure complete formation of benzoyl isothiocyanate reactant. Then, 6 mL aqueous solution of 2,5-difluorobenzene-1,4-diamine dihydrochloride (434 mg, 2 mmol) was added dropwise to the refluxing reaction mixture to precipitate thiourea derivatives. After the addition was completed, the reaction mixture was refluxed for 2 hours at 100 °C and filtered. The light yellow thiourea derivative was washed with acetone, water, and then acetone and dried under vacuum at room temperature.

The desulfurization procedure is the same as for H₂-PDCA and H₂-DC-PDCA. ^{1}H NMR (DMSO-d₆): δ = 7.06 (t, 2 H, CH$_{arom}$), 10.45 (br, 2 H, NH) ppm, IR: 3152 (N-H), 2236 (CN), 1531 (benzene ring). HRMS (ESI) calcd for $C_8H_4F_8N_2O_4S_2$ [M-H]$^-$: 406.95, found: 406.94.

Additional details are shown in **Figure S7**.

Lithiation of H₂-PDCA, H₂-DC-PDCA and H₂-DF-PDCA.

The lithiation of H₂-PDCA, H₂-DC-PDCA and H₂-DF-PDCA was performed in anhydrous methanol with a stoichiometric amount of lithium methoxide. The mixture was stirred at room temperature overnight in an argon-filled glove box. Then the solution was poured into excess of diethyl ether to precipitate a white product. The white precipitate was filtered and transferred to a BUCHI glass oven for drying. The Li₂-PDCA, Li₂-DC-PDCA, and Li₂-DF-PDCA were dried at 80 °C, 180 °C, 150 °C respectively, for 14 hours.

For Li₂-PDCA, ^{1}H NMR (DMSO-d₆): δ = 6.26 (s, 4 H, CH$_{arom}$) ppm, IR: 2117 (CN),

1502 (benzene ring).

For Li$_2$-DC-PDCA, ^{1}H NMR (DMSO-d$_6$): δ = 6.65 (s, 2 H, CH$_{arom}$) ppm, IR: 2124 (CN), 1472 (benzene ring).

For Li$_2$-DF-PDCA, ^{1}H NMR (DMSO-d$_6$): δ = 6.34 (t, 2 H, CH$_{arom}$) ppm, IR: 2150 (CN), 1505 (benzene ring).

Additional details are shown in **Figures S4-S7**.

Synthesis of N, N'-((1E, 4E)-2,5-dichlorocyclohexa-2,5-diene-1,4-diylidene) bis(1,1,1-trifluoromethanesulfonamide) (OX-DC-PDFSA)

To a solution of H$_2$-DC-PDFSA (0.25 mmol, 110.3 mg) in 3 ml glacial acetic acid, lead (IV) tetra acetate (0.35 mmol, 155 mg) was added under stirring, and a dark green suspension was obtained after 20 hours at room temperature. The powder was collected by filtration, washed with 7ml glacial acetic acid and dried under vacuum. ^{1}H NMR (CDCl$_3$-d): δ = 7.95 (s, 2 H, CH$_{quin}$) ppm, IR: 3036 (CH), 1584 (C=N), 1364, 1118 (SO$_2$).

Detailed information and comparisons with H$_2$-DC-PDFSA are shown in **Figure S8.**

Synthesis of (E, E)-N, N'-(2,5-dichlorocyclohexa-2,5-diene-1,4 diylidene) dicyanamide (OX-DC-PDCA)

Titanium tetrachloride (10.83 g, 57.14 mmol) in 8 ml anhydrous dichloromethane was added to a suspension of 2,5-dichlorocyclohexa-2,5-diene-1,4-dione (3.54 g, 20 mmol) in 15 mL anhydrous dichloromethane at 0°C under an argon atmosphere, and a red precipitate was observed immediately. Then the bis(trimethylsilyl) carbodiimide (9.32 g, 50 mmol) was rapidly added, and the mixture turned reddish. After 2 hours, the mixture was poured into 300 mL of cold water, and the organic phase was extracted with 400 mL of dichloromethane to create a transparent, reddish organic layer. After

dying with magnesium sulfate, the solution was concentrated and precipitated with petroleum ether to yield a yellow product. ^{1}H NMR (CDCl$_3$-d): $\delta = 7.78$ (s, 2 H, CH$_{quin}$) ppm, IR: 3034 (CH), 2180 (CN). The detailed information is shown in **Figure S9**.
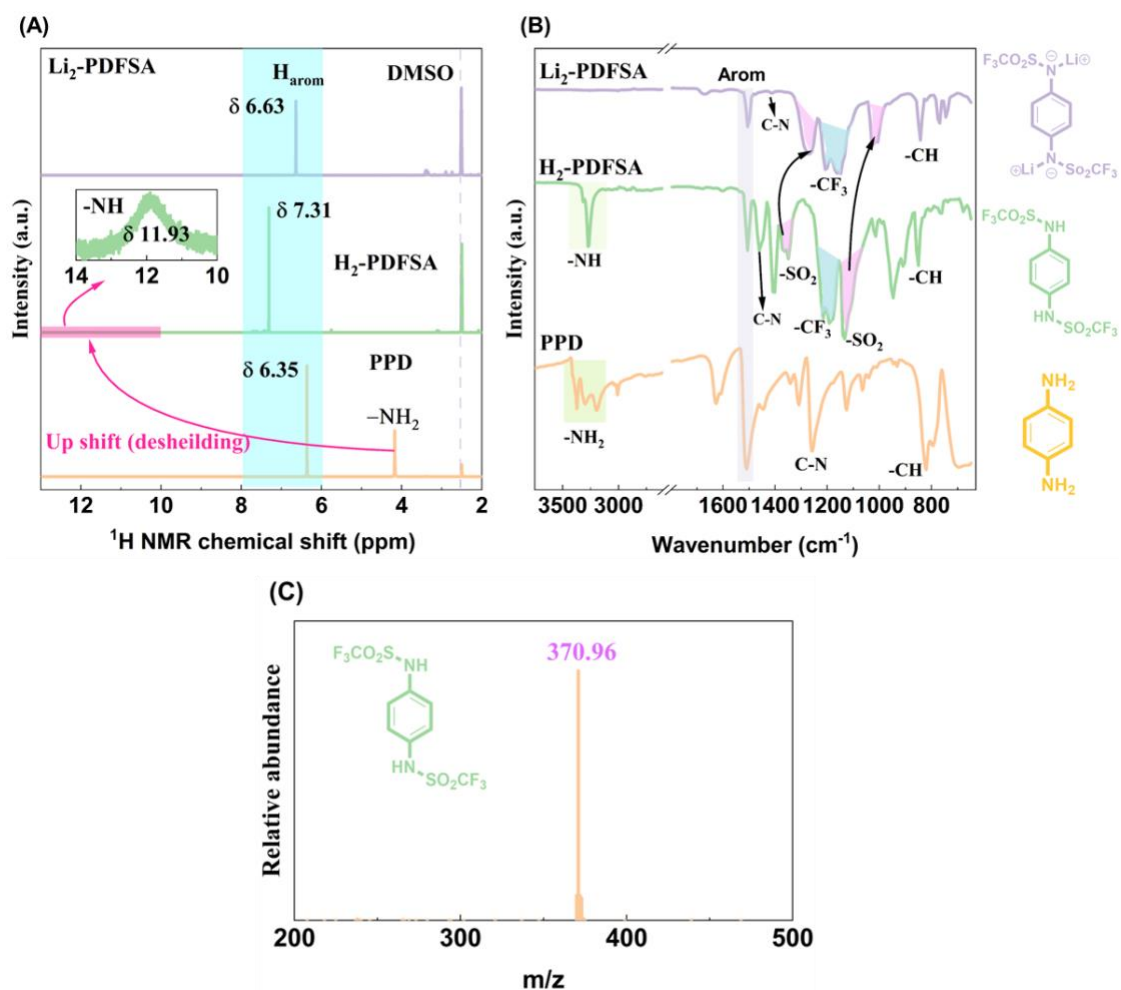
Figure S1. ^{1}H NMR spectra **(A)** and FTIR spectra **(B)** of the starting material p-Phenylenediamine (PPD), H_2-PDFSA and Li_2-PDFSA. HRMS spectrum of H_2-PDFSA **(C)**. The ^{1}H NMR, FTIR, and HRMS spectra demonstrate the successful preparation of the targeted materials.

Important features:

- In **Panel (A)**, the secondary amine protons in H_2-*p*-PDFSA are significantly de-shielded to 11.93 ppm, indicating their acidic nature. This is a result of the strong electron-withdrawing (EWG) effect of the trifluoromethanesulfonyl groups that decrease the electronic density over the N atom. The N-H proton signal disappears after H/Li exchange, accompanied by a slight shielding of aromatic protons.

- In **Panel (B)**, the primary amine bond ($\sim$3250 cm^{-1}) transforms into a secondary amine signatured by a sharp peak after grafting the triflimide group. In addition, trifluoromethyl band (1200 cm^{-1}) and two sulfonyl bands are also present. After lithiation, the characteristic FTIR N-H peak disappears, accompanied by a lower vibration frequency of the -SO$_2$ bonds due to the delocalization of the negative charges on the entire conjugated system.
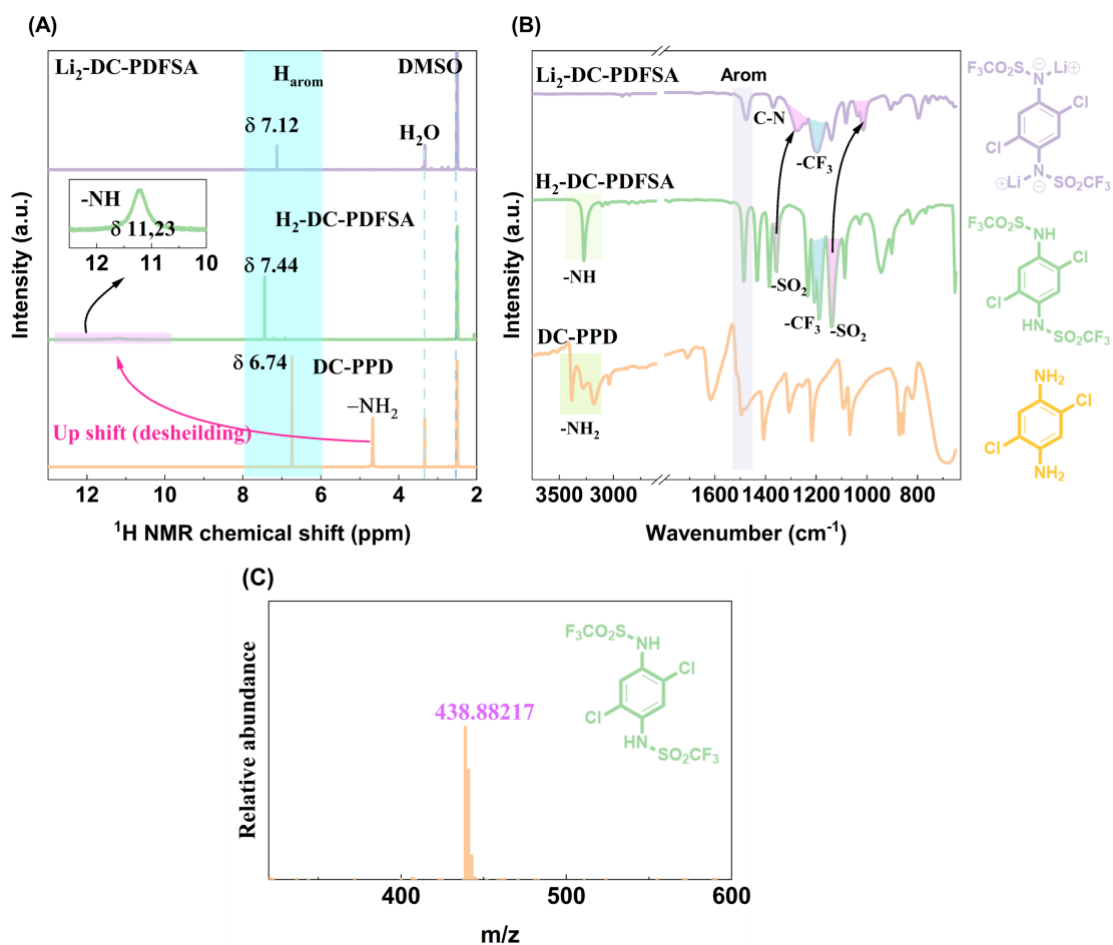
Figure S2. ^{1}H NMR spectra **(A)** and FTIR spectra **(B)** survey of the starting material 2,5-dichloro-1,4-phenylenediamine (DC-PPD), and of H_2-DC-PDFSA and Li_2-DC-PDFSA products. HRMS spectrum of H_2-DC-PDFSA **(C)**. The ^{1}H NMR, FTIR, and HRMS spectra demonstrate the successful preparation of the targeted materials.
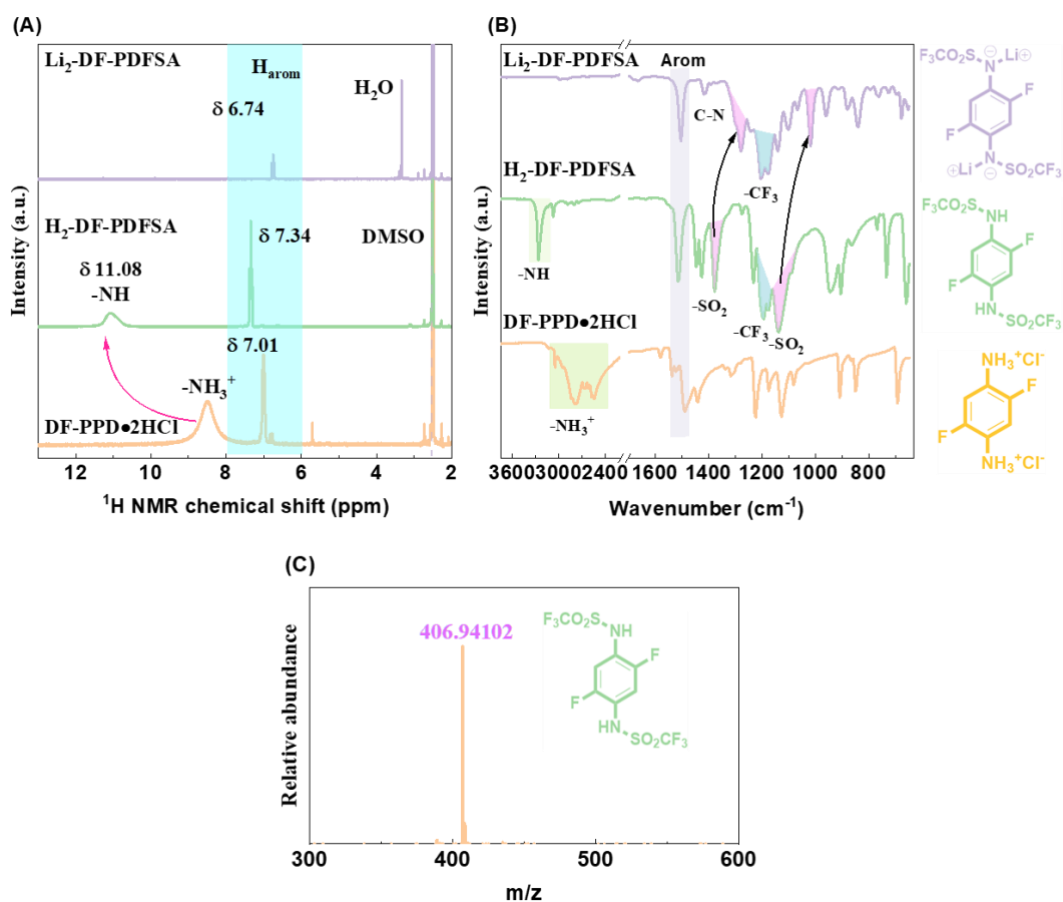
Figure S3. ^{1}H NMR spectra **(A)** and FTIR spectra **(B)** survey of the starting material 2,5-difluoro-1,4-phenylenediamine dihydrochloride (DF-PPD · 2HCl), and of H$_2$-DF-PDFSA and Li$_2$-DF-PDFSA products. HRMS spectra of H$_2$-DF-PDFSA **(C)**. The ^{1}H NMR, FTIR, and HRMS spectra demonstrate the successful preparation of the targeted materials.
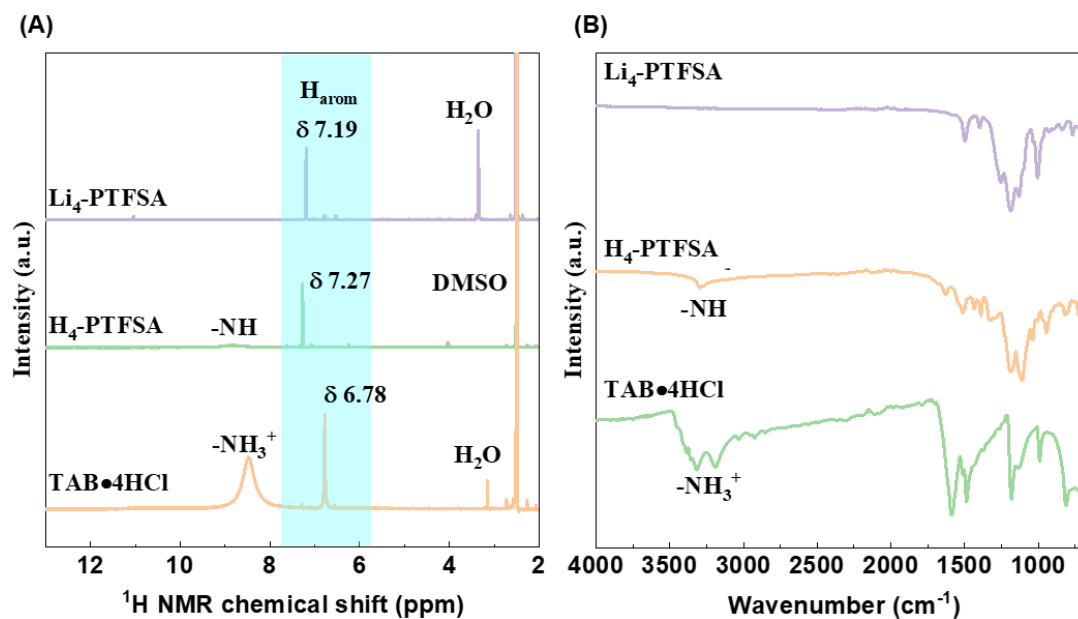
Figure S4. ^{1}H NMR spectra **(A)** and FTIR spectra **(B)** of the starting material 1,2,4,5-tetraaminobenzene tetrahydrochloride (TAB · 4HCl), and of H_4-PDFSA and Li_4-PDFSA products. The ^{1}H NMR and FTIR demonstrate the successful preparation of the targeted materials.

.
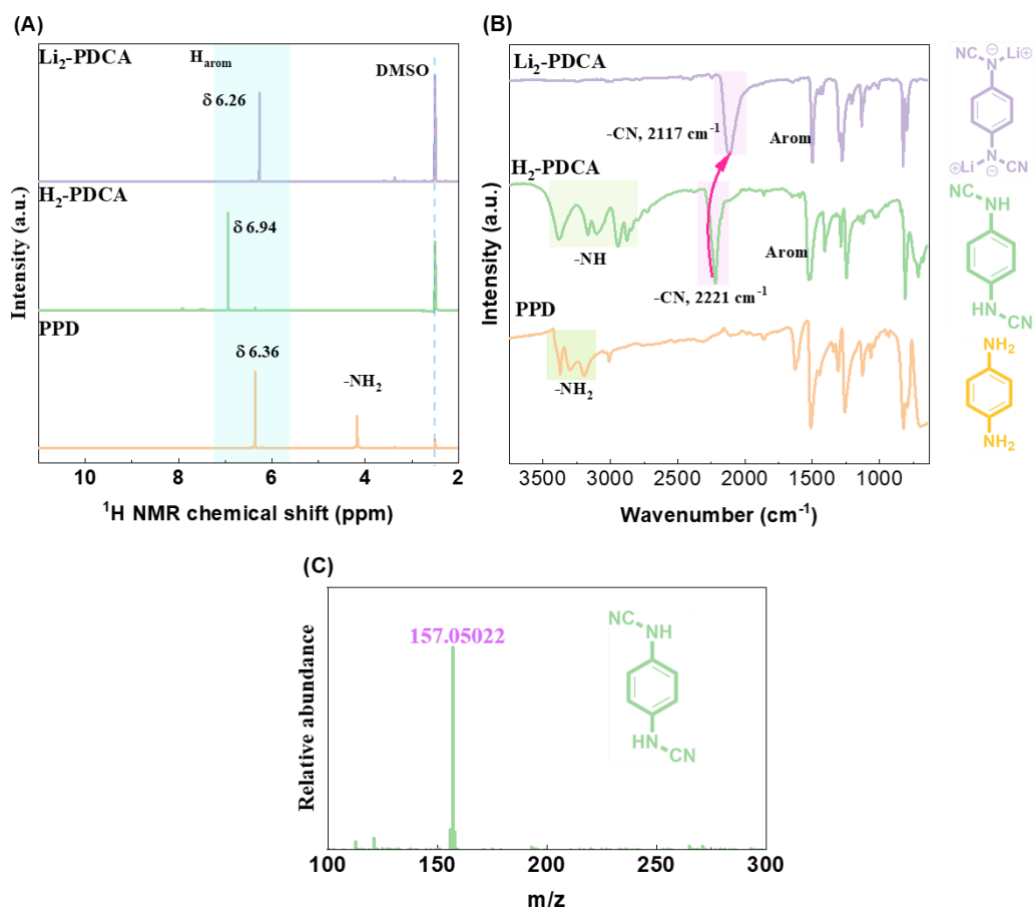
Figure S5. ^{1}H NMR spectra **(A)** and FTIR spectra **(B)** of the starting material PPD, and of prepared H$_2$-PDCA and Li$_2$-PDCA. HRMS spectrum of H$_2$-PDCA **(C)**.
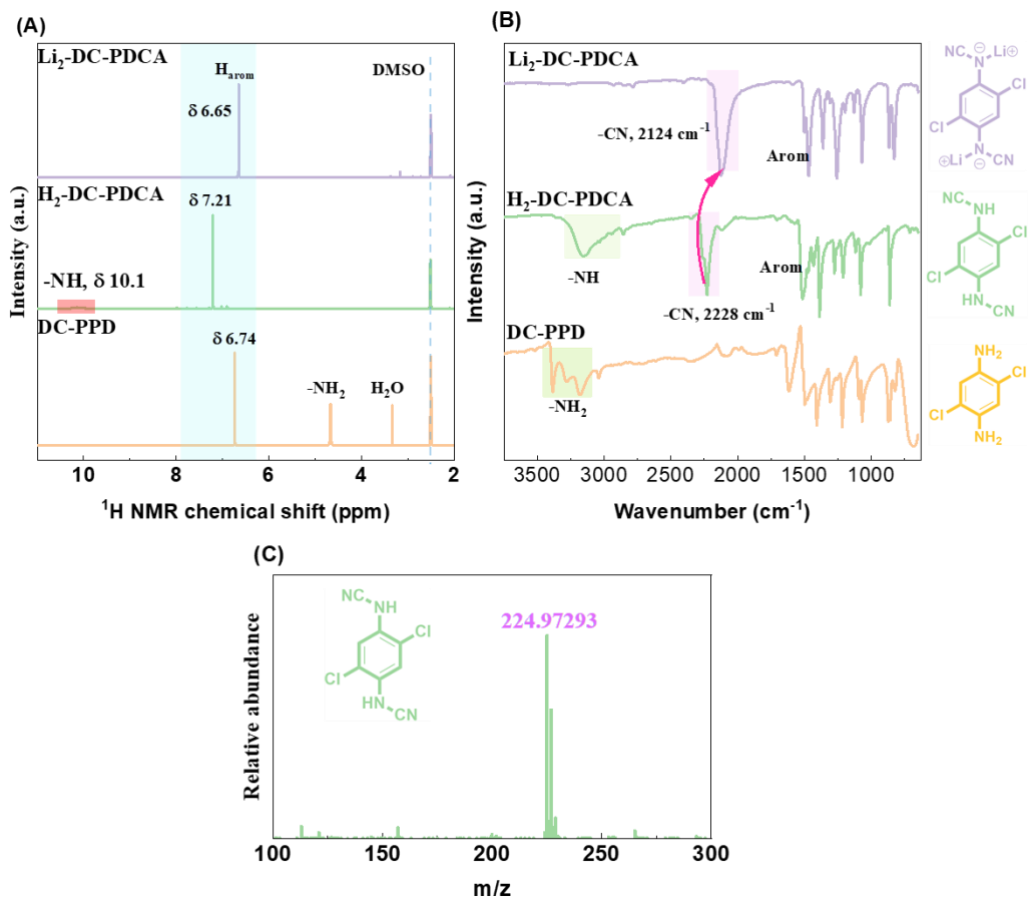
Figure S6. ^{1}H NMR spectra **(A)** and FTIR spectra **(B)** of the starting material DC-PPD, and of prepared H$_2$-DC-PDCA and Li$_2$-DC-PDCA. HRMS spectrum of H$_2$-DC-PDCA **(C).**
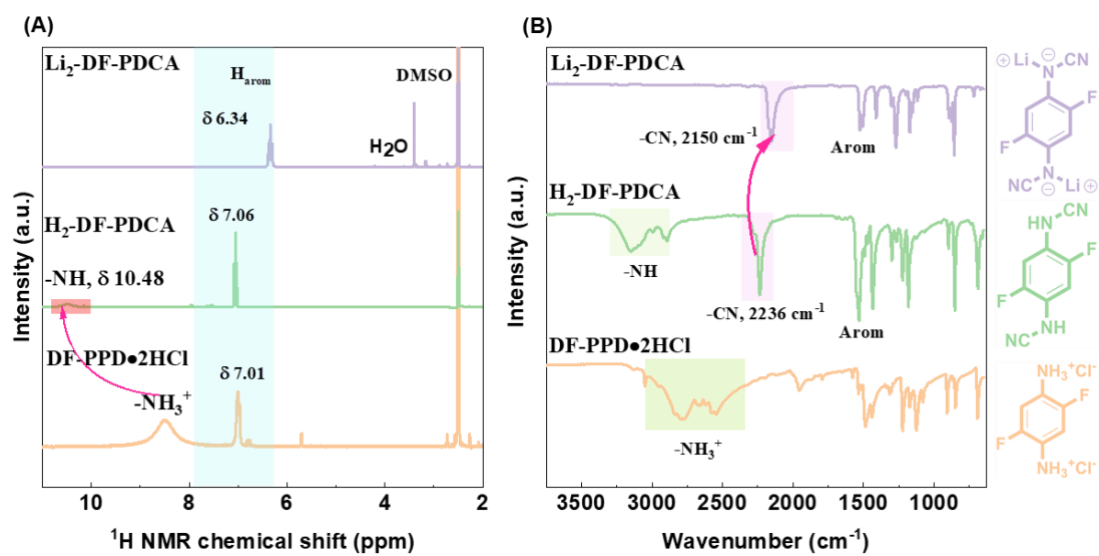
Figure S7. ^{1}H NMR spectra **(A)** and FTIR spectra **(B)** of the starting material DF-PPD · 2HCl, and of prepared H$_2$-DF-PDFSA and Li$_2$-DF-PDFSA.
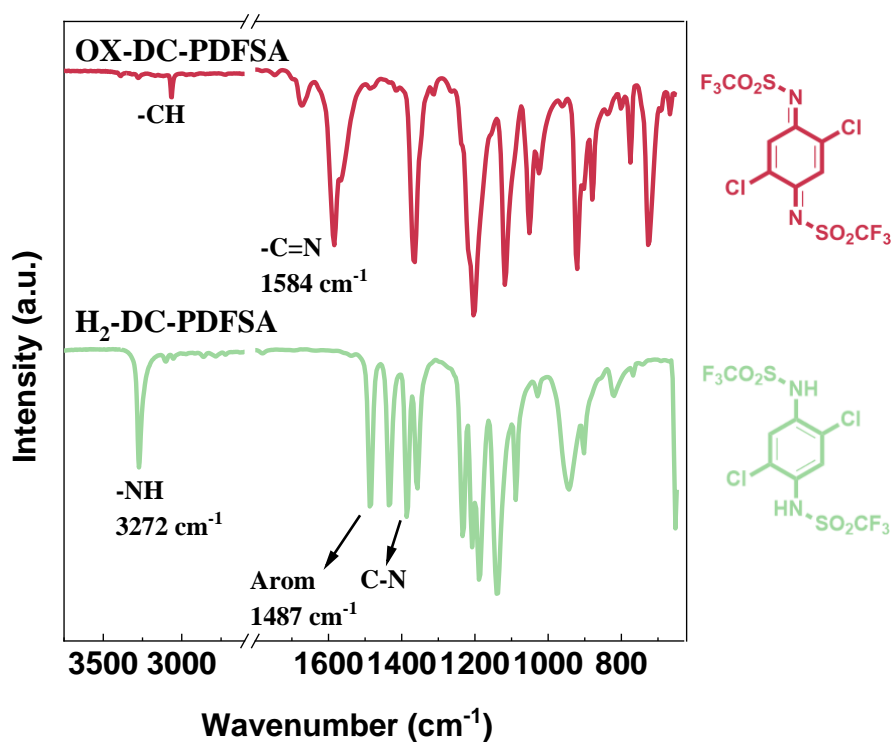
Figure S8. Comparative analyses of H_2-DC-PDFSA and OX-DC-PDFSA through FTIR spectra.

- The appearance of the strong imine vibration band ($\nu_{C=N}$ 1584 cm^{-1}) as well as the disappearance of the secondary amine (ν_{N-H} 3272 cm^{-1}) and the aromatic ring-stretching band (ν_{arom} 1487 cm^{-1}), both corroborate the formation of the quinoneimine form after oxidation.
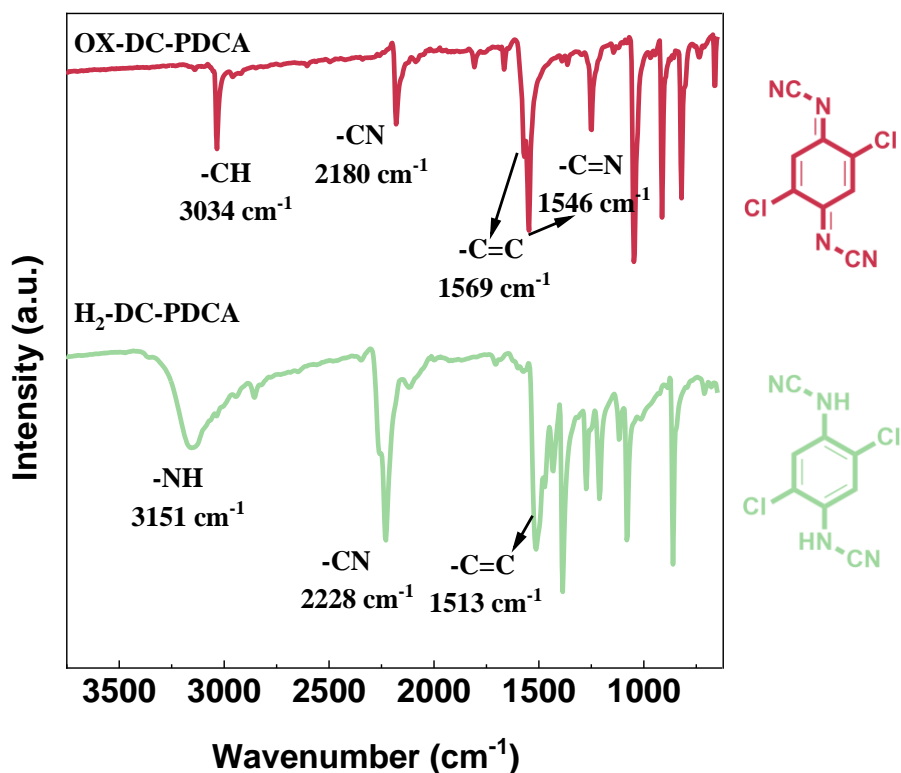
Figure S9. Comparative FTIR analysis of H_2-DC-PDCA and OX-DC-PDCA.

Important features:

- Appearance of the strong imine vibration band ($\nu_{C=N}$ 1546 cm^{-1}) as well as the disappearance of the secondary amine (ν_{N-H} 3151 cm^{-1}) and the aromatic ring-stretching band (ν_{arom} 1513 cm^{-1}), corroborate the formation of the quinoneimine form after oxidation.
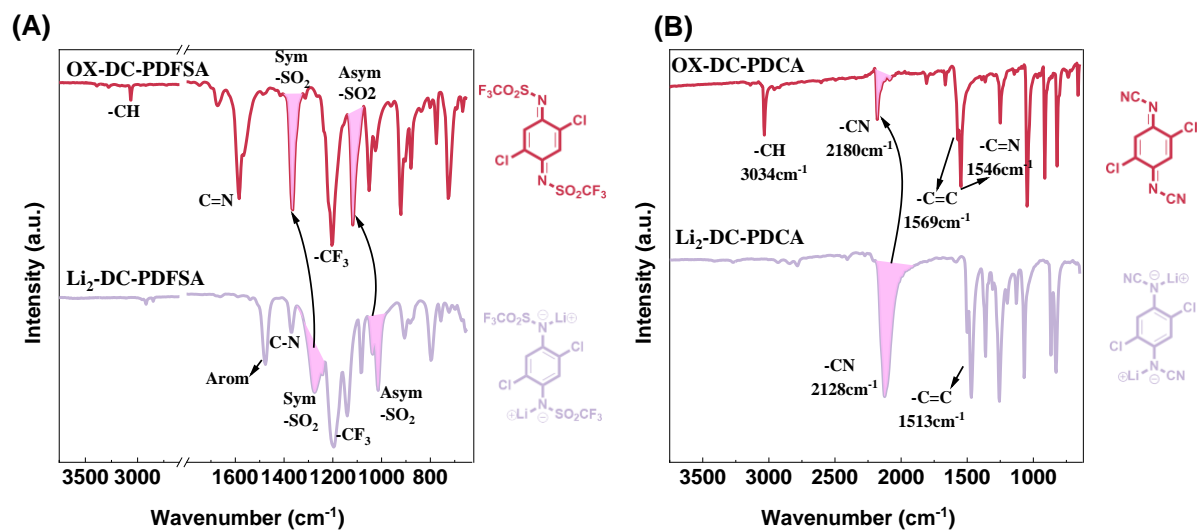
Figure S10. Comparative FTIR analyses of Li₂-DC-PDFSA - OX-DC-PDFSA **(A)** and of Li₂-DC-PDCA - OX-DC-PDCA **(B)** couples, respectively.

Electronic structure of *p*-Phenylenediamine, H$_2$-PDCA, and H$_2$-PDFSA.

Table S1. The molecular code, 2D representation, and the electrostatic potential maps.

Molecular code	2D representation	ESP map	
		Top view	Side view
p-Phenylenediamine			
H$_2$-PDCA			
H$_2$-PDFSA			
		-0.15 a.u.　　　　　　0.15 a.u.	
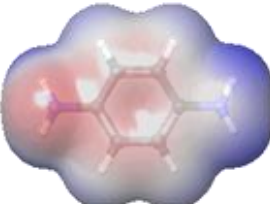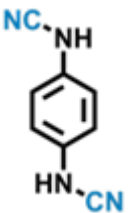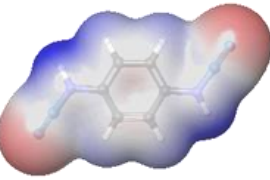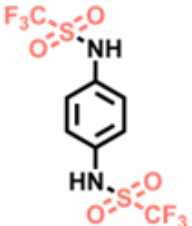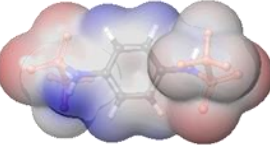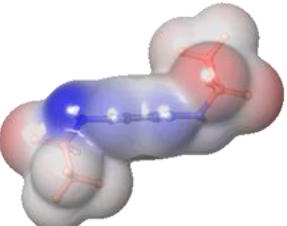
The electronic structure calculations of *p*-Phenylenediamine, H$_2$-PDCA, and H$_2$-PDFSA were performed to investigate the effect of introduced electron-withdrawing groups –SO$_2$CF$_3$ and –CN on charge distribution. In the ESP maps, the red and blue regions represent negative and positive charges, respectively, and darker color indicates higher charge density. For the ESP visualizations, the isosurface value was set at 0.01 a.u.

The ESP map of *p*-phenylenediamine exhibits a preponderance of red color in the aromatic ring and nitrogen atoms, indicating that electron are localized near these atoms.

Meanwhile, it can be observed that the electron density of aromatic ring and nitrogen atoms decreases for H_2-PDCA and H_2-PDFSA. It indicates that the introduction of the –CN and –SO_2CF_3 groups results in electron transfer from aromatic rings and nitrogen atoms to EWGs.
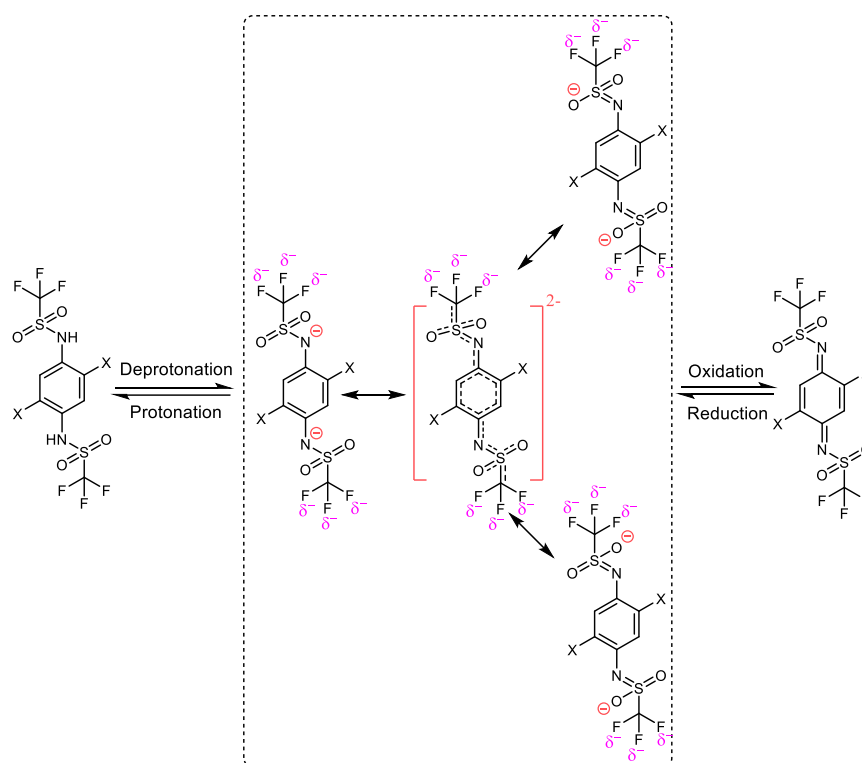
Figure S11. Schematic representation of the conjugation and mesomeric effects in the triflimides chemistry. X = H, Cl, or F.
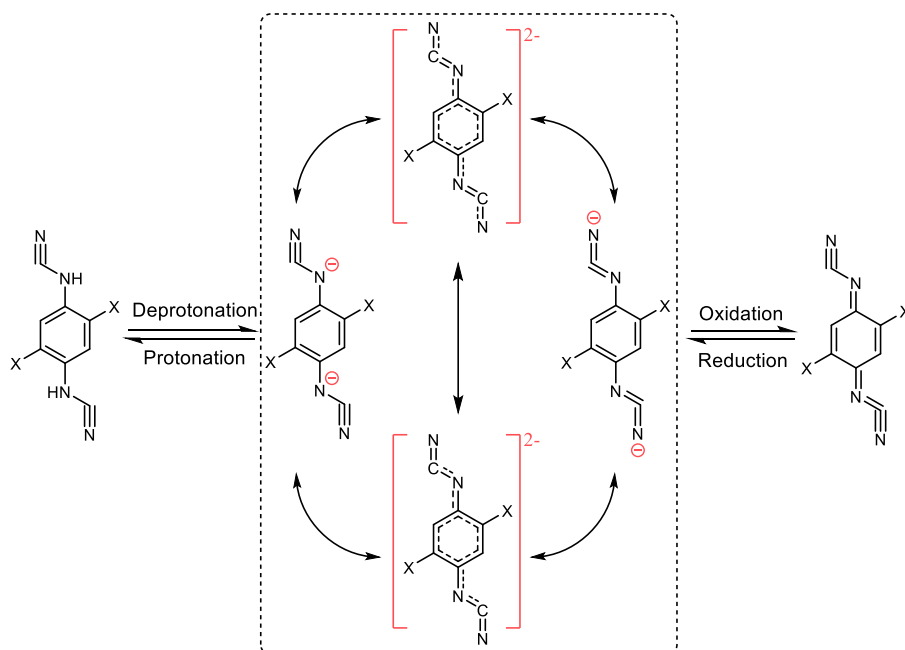
Figure S12. Schematic representation of conjugation and mesomeric effect in the cyanamides chemistry. X=H, Cl, or F.
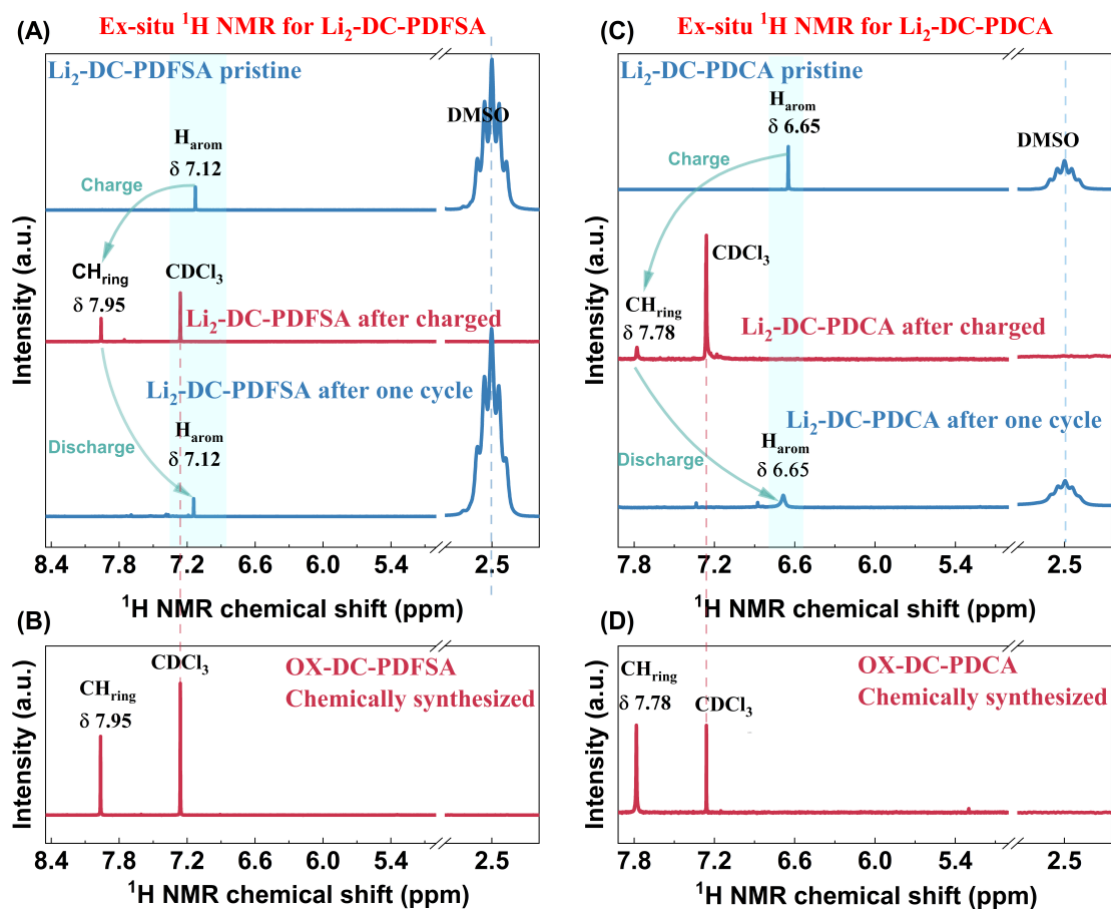
Figure S13. Ex-situ ^{1}H NMR spectra of the electrochemically oxidized (charged) and reduced (discharged) states of Li$_2$-DC-PDFSA **(A)** and Li$_2$-DC-PDCA **(C)**; compared to chemically oxidized OX-DC-PDFSA **(B)** and OX-DC-PDCA **(D)**.
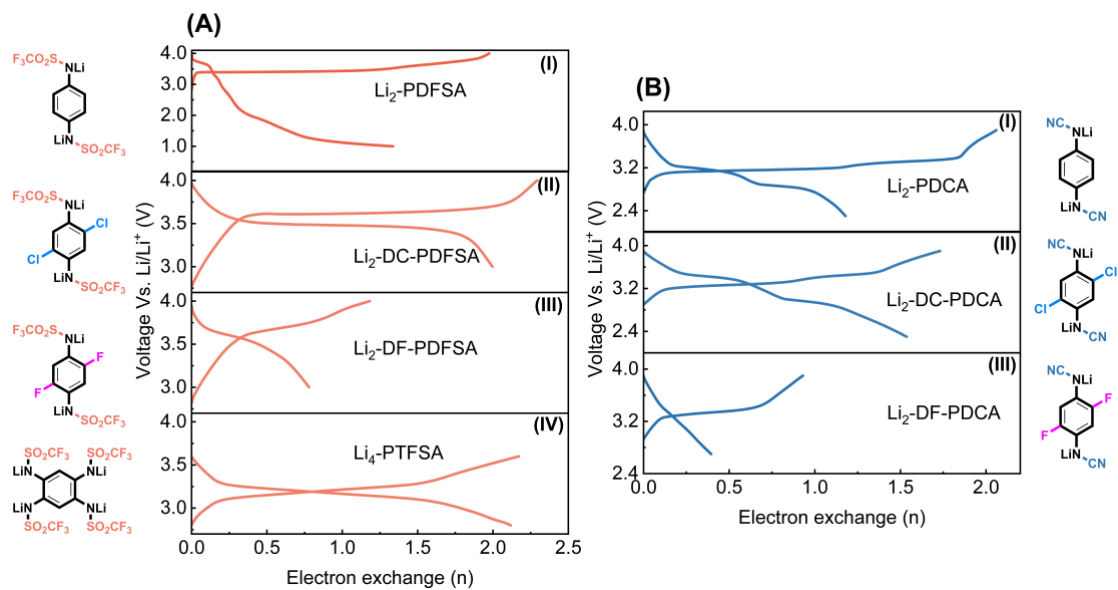
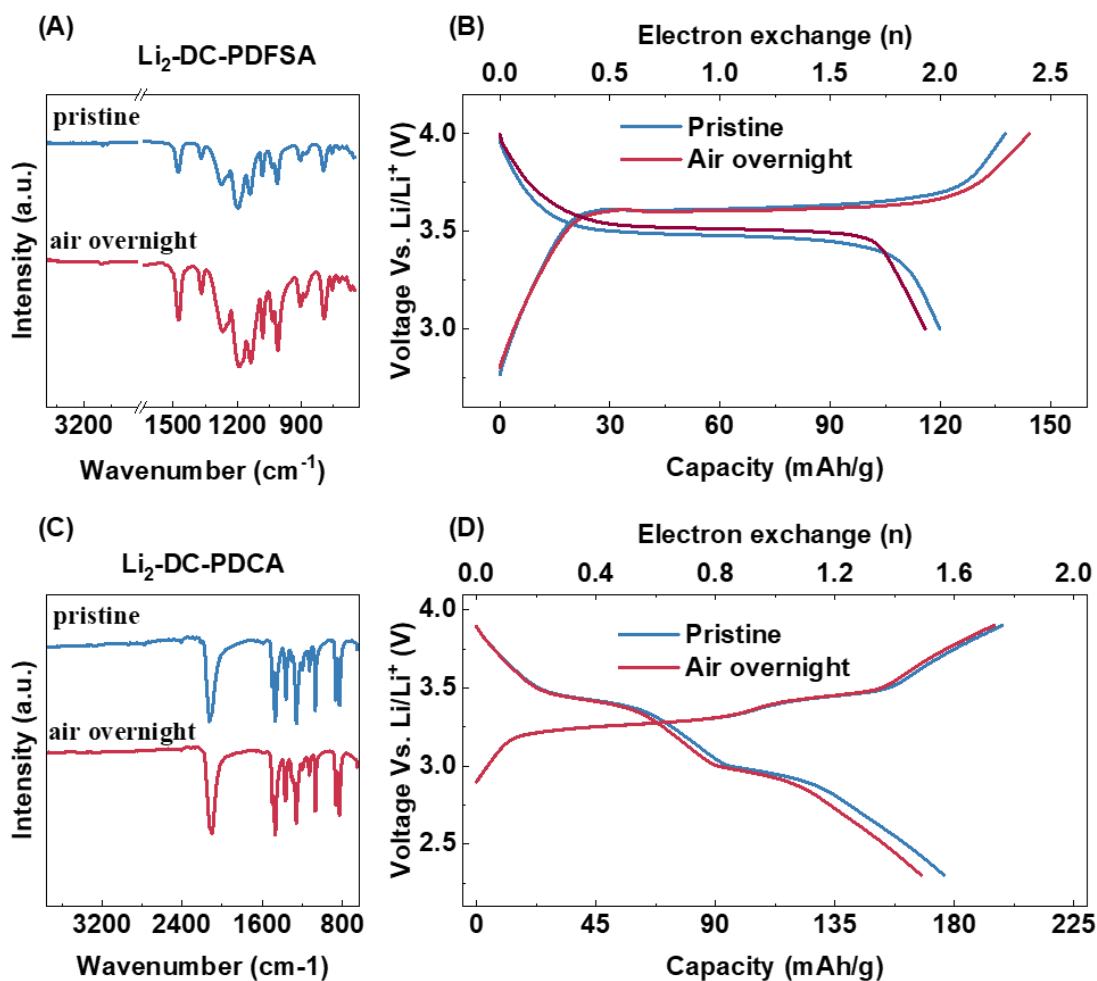**Figure S14.** First cycle of galvanostatic charge/discharge profiles of triflimides **(A)** and cyanamides **(B)** in Li half-cell.

Figure S15. Air stability of Li$_2$-DC-PDFSA and Li$_2$-DC-PDCA materials. FTIR **(A, C)** and charge-discharge galvanostatic plots **(B, D)** of pristine Li$_2$-DC-PDFSA and Li$_2$-DC-PDCA respectively, after being exposed to ambient air.

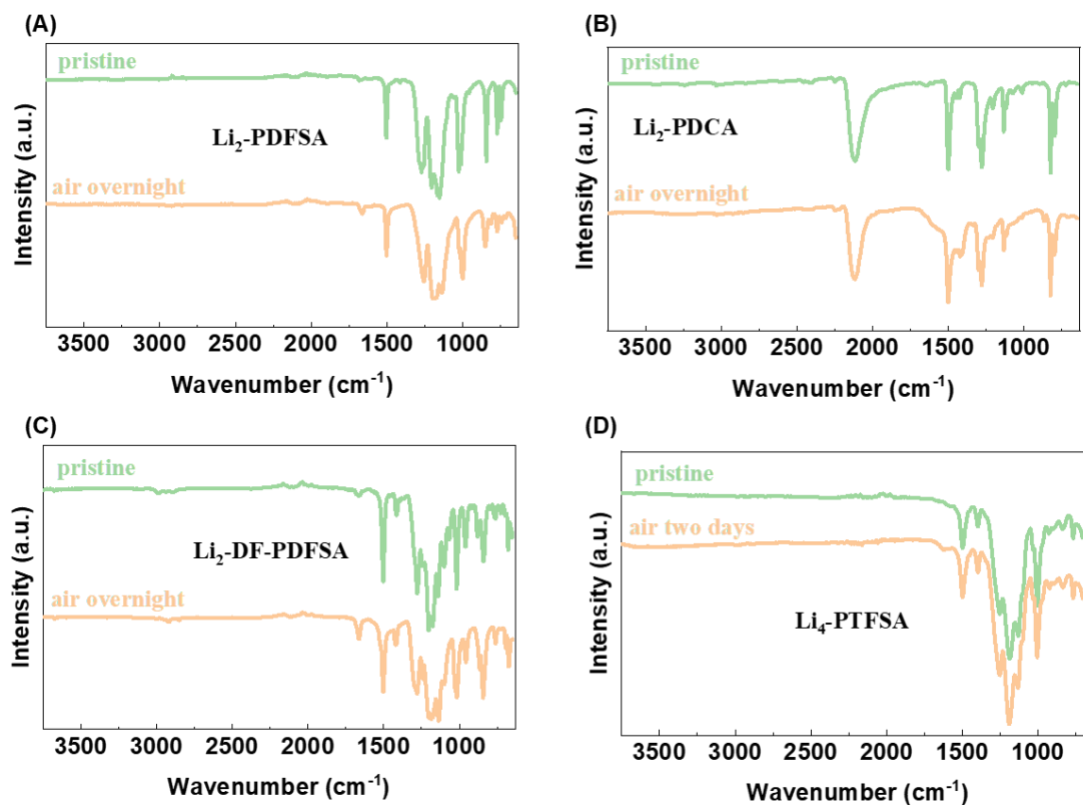**Figure S16**. Air stability FTIR analysis of Li$_2$-PDFSA (**A**), Li$_2$-PDCA (**B**), Li$_2$-DF-PDFSA (**C**), and Li$_4$-PTFSA (**D**).

The stability of triflimides and cyanamides under ambient conditions was investigated. The enhanced stability can be explained by the following: the mesomeric (+M) and inductive (-I) effects increase the oxidation potential beyond 2.91 V vs. Li$^+$/Li^0 limit, thereby rendering them resistant to oxidation by oxygen. Furthermore, negative charges in triflimides and cyanamides are delocalized from the nitrogen center over conjugation systems (**Figure S11 and S12**). This phenomenon results in a reduction of nucleophilicity making them resistant to hydrolysis (proton trapping). Detailed solid electrochemical performances and FTIR spectra for triflimides and cyanamides exposed to air are presented in **Figures S15** and **S16**, respectively.
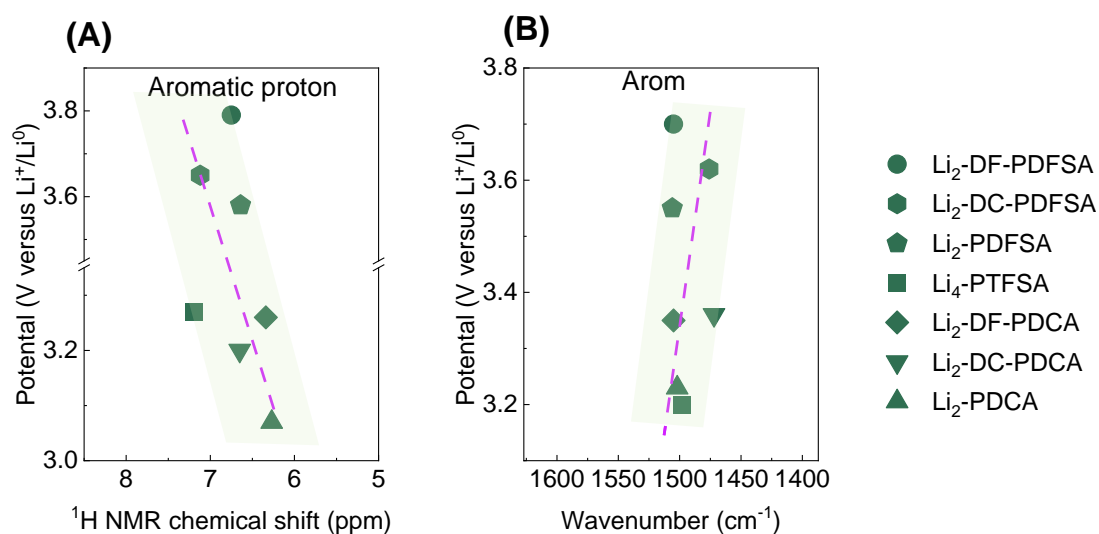
Figure S17. Correlation between the ^{1}H NMR chemical shift of aromatic protons **(A)** and corresponding aromatic FTIR bands **(B)** with the delithiation potential of the studied compounds.
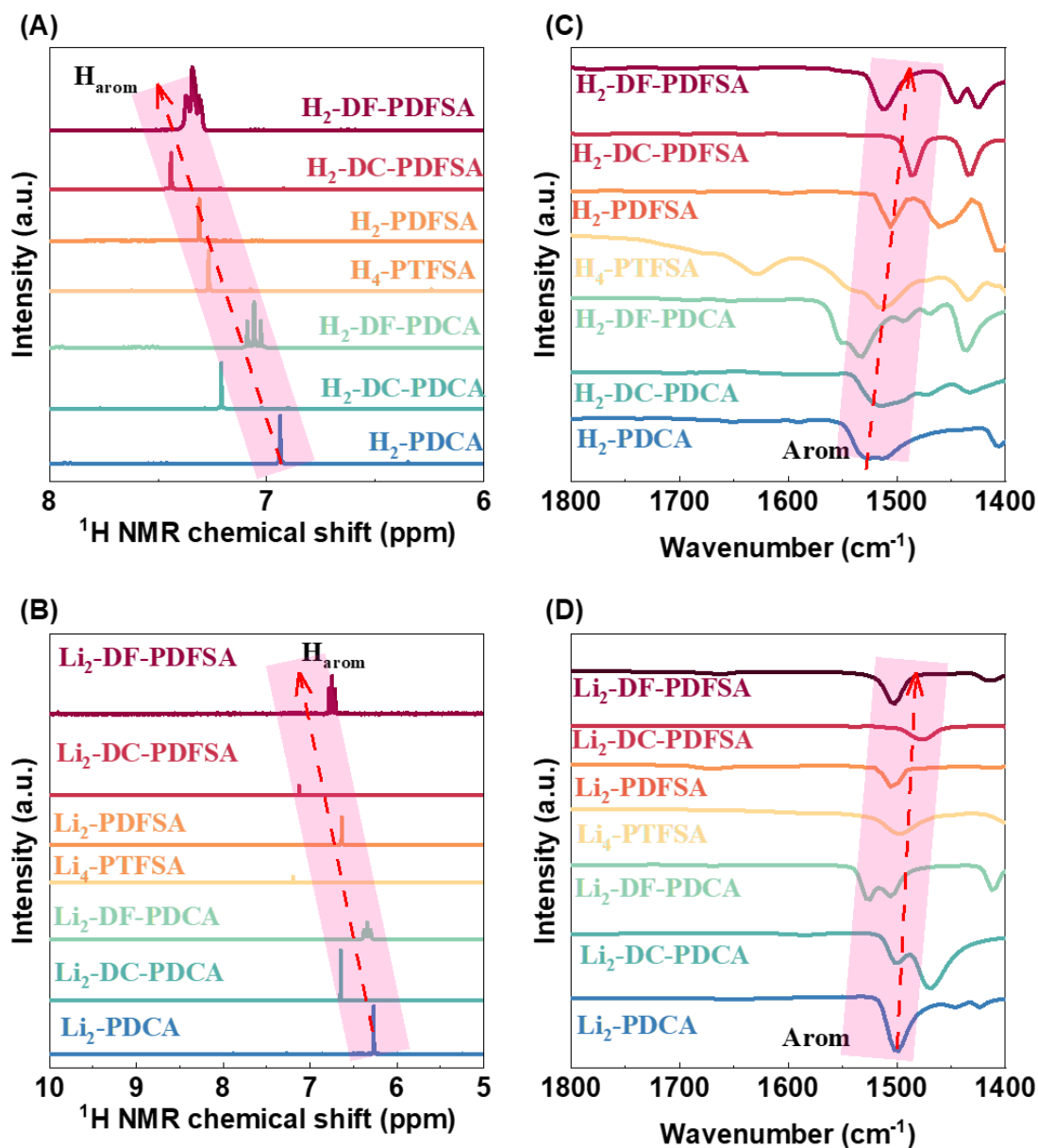
Figure S18. ^{1}H NMR spectra of pronated and lithiatied triflimides and cyanamides **(A, B)** and FTIR spectra of pronated and lithiatied triflimides and cyanamides **(C, D)**, highlighting the characteristic peak shift.
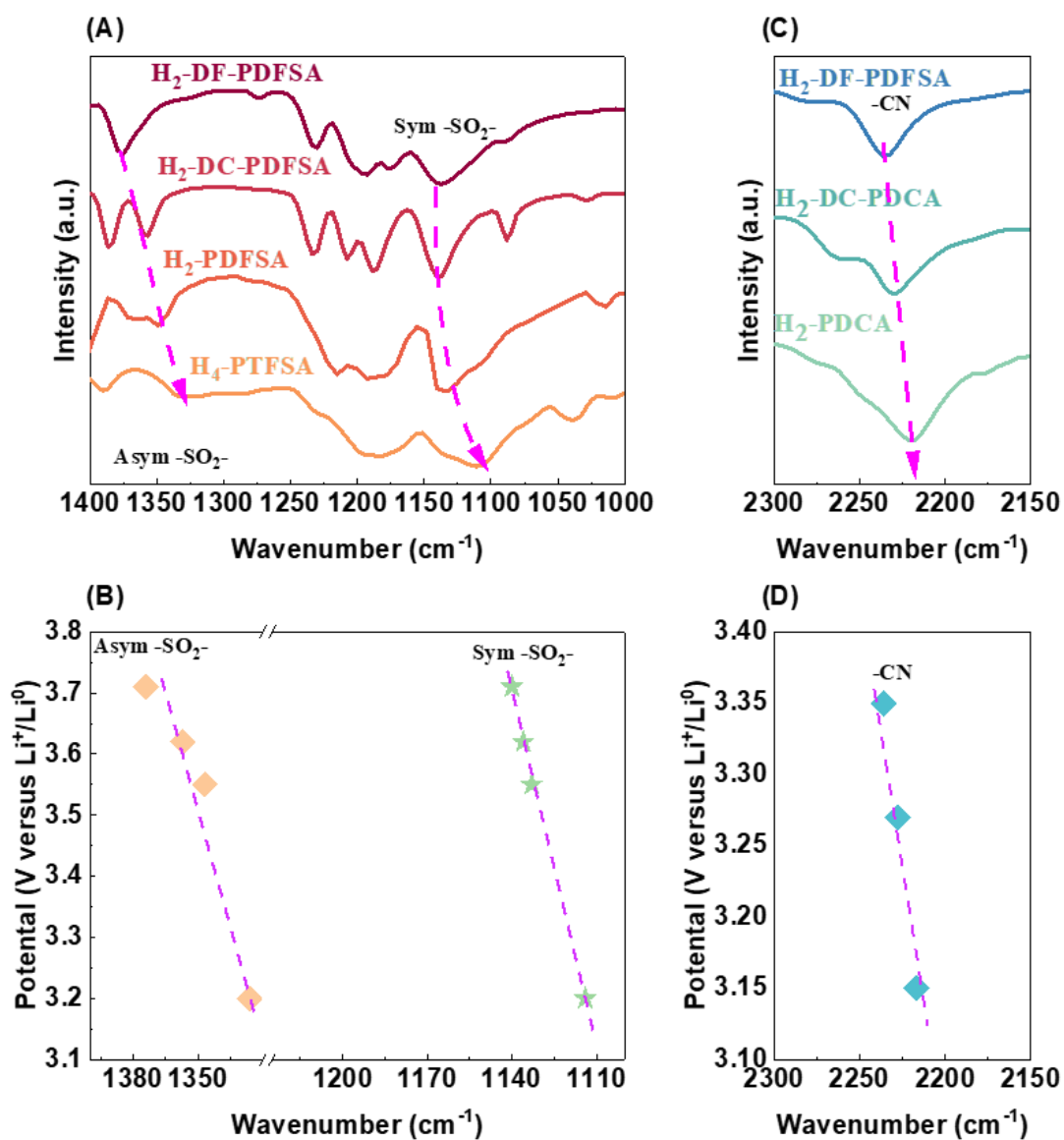
Figure S19. FTIR spectra of protonated triflimides (**A**) and cyanamides (**C**) and the correlation between the vibration frequency of specific bands and their averaged redox potential (**B, D**).
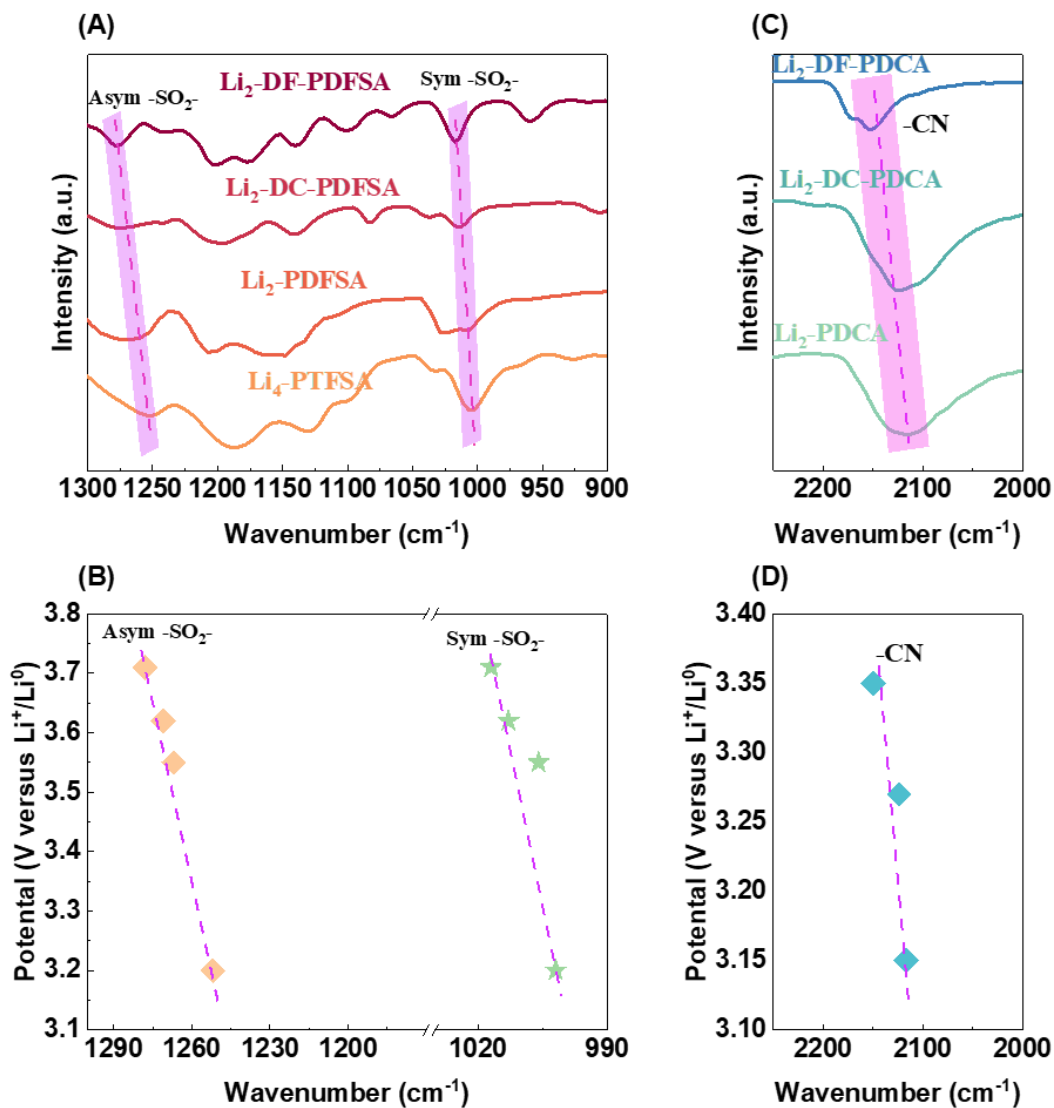
Figure S20. FTIR spectra of lithiated triflimides (**A**) and cyanamides (**C**) and the correlation between the vibration frequency of specific bands and their averaged redox potential (**B, D**).
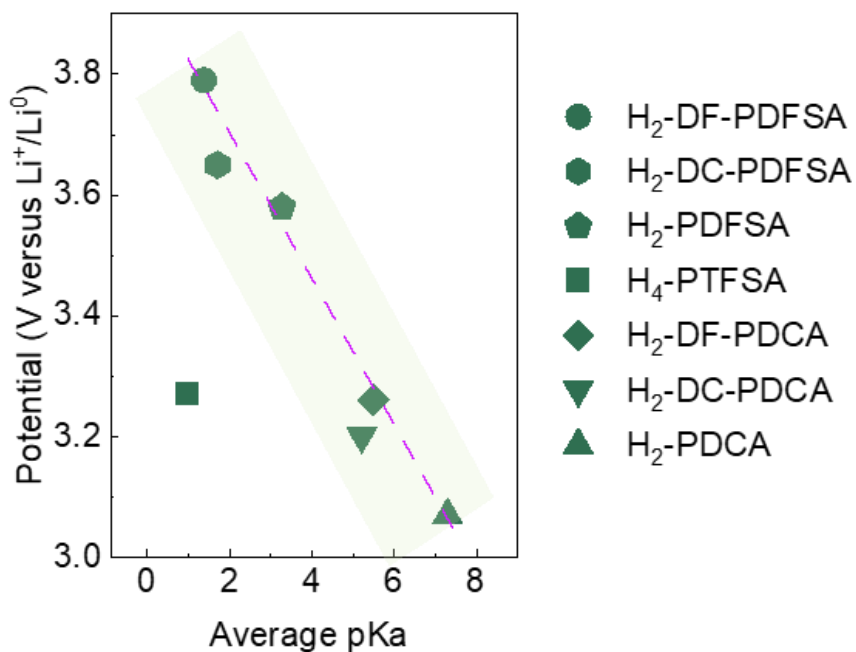
Figure S21. Correlation between the average pKa values of imine H atoms and the delithiation potential of studied materials. Here, H4-PTFSA is out of trend because it contains four acidic protons that can be dissociated, while the other compositions have only two acidic protons that can be dissociated.
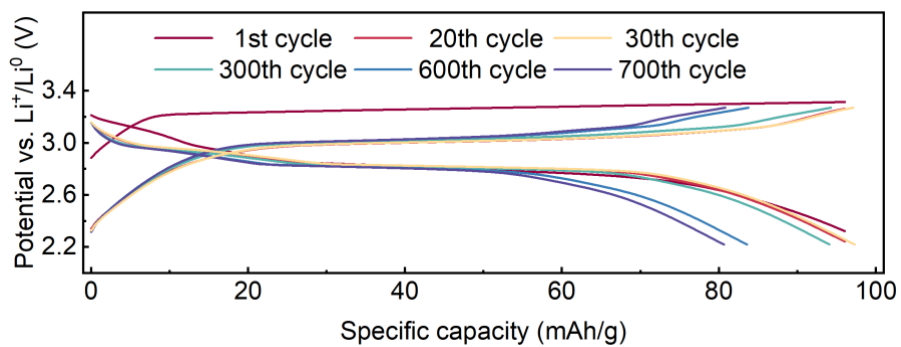
Figure S22. Galvanostatic charge/discharge profiles of Li$_2$-PDCA limited to 0.6 - electron capacity for different cycle numbers.
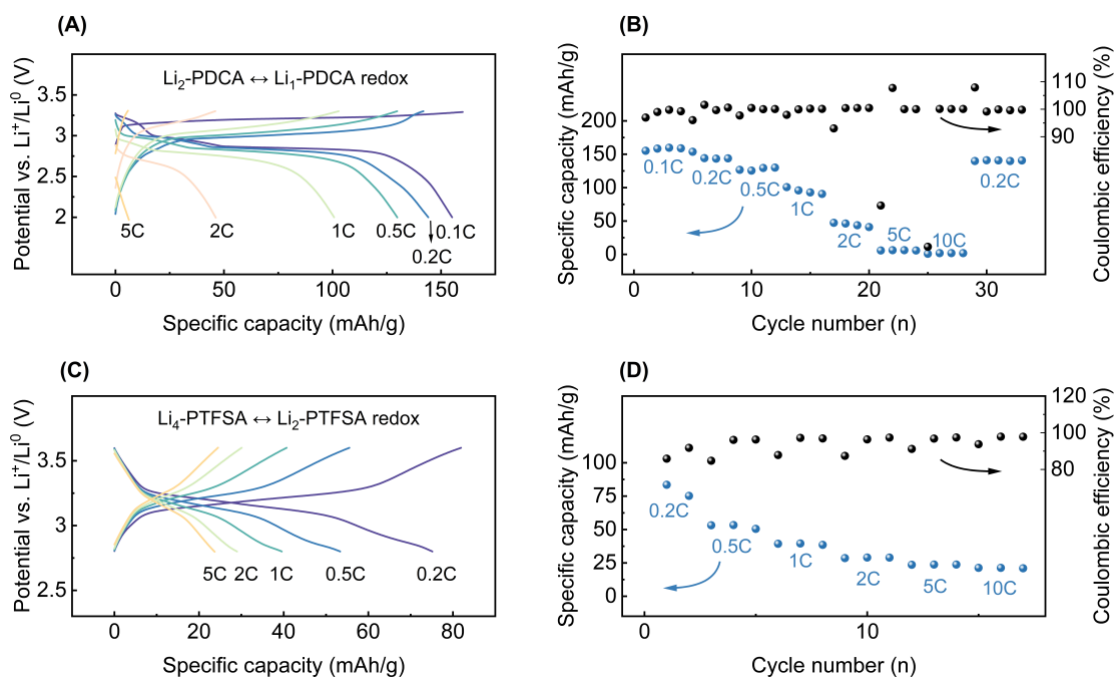
Figure S23. (A) Galvanostatic charge/discharge profiles of Li_2-PDCA restricted to 1 - electron capacity for various C-rate measurements and **(B)** corresponding capacity retention at different cycling rates. **(C)** Galvanostatic charge/discharge profiles of Li_4-PTFSA for various C-rate measurements and **(D)** corresponding capacity retention at different cycling rates.

SI References:

1   User Manual Schrödinger, *Inc., New York NY*.

2   K. Roos, C. J. Wu, W. Damm, M. Reboul, J. M. Stevenson, C. Lu, M. K. Dahlgren, S. Mondal, W. Chen, L. L. Wang, R. Abel, R. A. Friesner and E. D. Harder, OPLS3e: Extending force field coverage for drug-like small molecules, *J. Chem. Theory Comput.*, 2019, **15**, 1863–1874.

3   F. Mohamadi, N. G. J. Richards, W. C. Guida, R. Liskamp, M. Lipton, C. Caufield, G. Chang, T. Hendrickson and W. C. Still, MacroModel - An integrated software system for modeling organic and bioorganic molecules using molecular mechanics, *J. Comput. Chem.*, 1990, **11**, 440–467.

4   S. M. Bachrach, Jaguar 5.5, *J. Am. Chem. Soc.*, 2004, **126**, 5018.

5   S. T. Schneebell, A. D. Bochevarov and R. A. Friesner, Parameterization of a B3LYP specific correction for non-covalent interaction and basis set superposition error on a gigantic dataset of CCSD(T) quality non-covalent interaction energies, *J. Chem. Theory Comput.*, 2011, **7**, 658–668.

6   P. J. Hay and W. R. Wadt, Ab initio effective core potentials for molecular calculations. Potentials for K to Au including the outermost core orbitals, *J. Chem. Phys.*, 1985, **82**, 299–310.

7   A. D. Bochevarov, E. Harder, T. F. Hughes, J. R. Greenwood, D. A. Braden, D. M. Philipp, D. Rinaldo, M. D. Halls, J. Zhang and R. A. Friesner, Jaguar: A high-performance quantum chemistry software program with strengths in life and materials sciences, *Int. J. Quantum Chem.*, 2013, **113**, 2110–2142.

8   B. Marten, K. Kim, C. Cortis, R. A. Friesner, R. B. Murphy, M. N. Ringnalda, D. Sitkoff and B. Honig, New model for calculation of solvation free energies: Correction of self-consistent reaction field continuum dielectric theory for short-range hydrogen-bonding effects, *J. Phys. Chem.*, 1996, **100**, 11775–11788.

9   Aquino M A S, Lee F L, Gabe E J, et al. Superexchange metal-metal coupling in dinuclear pentaammineruthenium complexes incorporating a 1, 4-dicyanamidobenzene dianion bridging ligand[J]. Journal of the American Chemical Society, 1992, 114(13): 5130-5140.